NUCL SCI TECH (2016) 27:151
DOI 10.1007/s41365-016-0152-0

QCD phase diagram with the improved Polyakov loop effective potential

Guo-Yun Shao[1] · Xue-Yan Gao[1] · Zhan-Duo Tang[1] · Ning Gao[1]

Received: 12 August 2016 / Revised: 15 October 2016 / Accepted: 15 October 2016 / Published online: 31 October 2016

Abstract We report our recent progress on the QCD phase structure. We explore the properties of quark–gluon matter in the improved Polyakov–Nambu–Jona–Lasinio (PNJL) model by introducing a chemical potential-dependent Polyakov loop potential. This treatment effectively reflects the quantum backreaction of matter sector to glue sector at nonzero chemical potential. Compared with the original PNJL model, a superiority of the improved PNJL model is that it can effectively describe the confinement–deconfinement transition at low temperature and high density. And the QCD phase diagram will be modified to a certain degree if the strength of the quantum backreaction of matter sector to glue sector is strong. One evident variation is that the region of quarkyonic phase will be greatly reduced in the improved PNJL model. This means that the modification to the Polyakov loop potential with the chemical potential dependence is possibly a significant improvement in exploring the full QCD phase structure.

Keywords QCD phase diagram · Chiral symmetry · Confinement–deconfinement phase transition

1 Introduction

Exploring the QCD phase diagram of strongly interacting matter and searching for phase transition signatures from nuclear to quark–gluon matter are subjects of great interest. Recently, intensive searches on high-energy heavy-ion collision (HIC) have been performed in laboratories such as RHIC and LHC, and a near perfect fluid of quark–gluon plasma (QGP) has been created [1]. To look for the critical end point and the boundaries of the phase transition, more experiments are in plan on the next generation facilities such as the second stage of beam energy scan (BES II) project on RHIC and programs on NICA/FAIR/J-PARC. In particular, experiments will be performed in the region of high baryon density where a promising observation of the signatures of the phase transformation is being looked forward to. Ultimately, these phenomena need to be understood in the frame of quantum chromodynamics (QCD). However, in spite of tremendous theoretical and experimental efforts, the QCD phase diagram has not been unveiled yet [2, 3]. Lattice QCD simulation is very successful in investigating the thermodynamics of QCD matter at vanishing and/or small chemical potential [4–9], but the situation is not clear at large chemical potential μ_B since lattice QCD suffers the sign problem of the fermion determinant with three colors at finite baryon chemical potential. Although some approximation methods have been proposed to try to overcome the problem, the region of large chemical potential and low temperature essentially remains inaccessible [10–12].

Complementary to lattice QCD simulation, some quantum field theory approaches and phenomenological models, such as the Dyson–Schwinger equation approach [13, 14],

This work was supported by the National Natural Science Foundation of China (No. 11305121), the Specialized Research Fund for the Doctoral Program of Higher Education (No. 20130201120046), the Natural Science Basic Research Plan in Shanxi Province of China (No. 2014JQ1012) and the Fundamental Research Funds for the Central Universities.

✉ Guo-Yun Shao
gyshao@mail.xjtu.edu.cn

[1] Department of Applied Physics, Xi'an Jiaotong University, Xi'an 710049, China

the Nambu–Jona–Lasinio (NJL) model [15–19], the PNJL model [20–22], the entanglement extended PNJL (EPNJL) model [23], the Polyakov loop extended quark–meson (PQM) model [24–26], the enhanced pQCD model [27], and the equivparticle model [28, 29] have been developed to describe the properties of quark matter.

Among these models, the PNJL model, which takes into account both the chiral dynamics and (de)confinement effect at high temperature, gives a good reproduction of lattice data at vanishing chemical potential. On the other hand, in the original PNJL model, a "quarkyonic phase" in which quarks are confined, but the dynamical chiral symmetry is already restored appears at high density and finite temperature [30, 31]. In theory, quark deconfinement should also occur at high density. The absence of quark deconfinement at low T and high density in the original PNJL model originates from the Polyakov loop potential is extracted from pure Yang–Mills lattice simulation at vanishing. In the presence of dynamical quarks, the contribution from matter sector and its quantum backreaction to the glue sector should be included. This was realized by introducing a flavor and chemical potential-dependent Polyakov loop potential in the functional renormalization group (FRG) approach [32]. Therefore, with the incorporation of both the matter and glue dynamics, the flavor and chemical potential-dependent Polyakov loop potential should be taken in to study the QCD phase transition and thermodynamics [32–38].

As a further study along this line, we take a chemical potential-dependent Polyakov loop potential in the PNJL model to explore the relation between quark condensate and Polyakov loop dynamics and investigate the full QCD phase diagram. Compared with the results derived in the original PNJL model, the calculation presents that, with the inclusion of the backreaction of matter sector to glue sector, the deconfinement phase transition line moves toward low temperature at large chemical potential. The critical end point of the first-order phase transition moves toward low T and large μ_B in the QCD phase diagram. The transition region near by the critical end point is possibly reached in the planed experiments at the facilities of NICA/FAIR/J-PARC and BES II program at RHIC. The future heavy-ion-collision experiments will provide us some hints on the QCD phase structure.

The paper is organized as follows. In Sect. 2, we describe briefly the improved PNJL model with the inclusion of quantum backreaction of matter sector to glue sector at finite chemical potential and give the relevant formulas. In Sect. 3, we present the full QCD phase diagram in the improved PNJL model, and analyze the influence of the μ-dependent Polyakov loop potential on the chiral and deconfinement phase transition. Finally, a summary is given in Sect. 4.

2 Theoretical descriptions

To describe the properties of quark matter first, we introduce the standard two-flavor PNJL model and then consider the μ-dependent Polyakov loop potential which reflects the quantum backreaction of matter sector to glue sector at nonzero quark chemical potential. The Lagrangian of the standard two-flavor PNJL model is

$$\begin{aligned}\mathcal{L}^{\mathcal{Q}} &= \bar{q}(i\gamma^{\mu}D_{\mu}-\hat{m}_0)q+G\left[(\bar{q}q)^2+(\bar{q}i\gamma_5\vec{\tau}q)^2\right]\\ &\quad-\mathcal{U}(\Phi[A],\bar{\Phi}[A],T),\end{aligned} \tag{1}$$

where q denotes the quark fields with two flavors, u and d, and three colors ($\hat{m}_0 = \mathtt{diag}(m_u,\ m_d)$ in flavor space). The covariant derivative in the Lagrangian is defined as $D_{\mu} = \partial_{\mu} - iA_{\mu} - i\mu_q\delta^0_{\mu}$. The glue background field $A_{\mu} = \delta^0_{\mu}A_0$ is supposed to be homogeneous and static, with $A_0 = g\mathcal{A}^{\alpha}_0\frac{\lambda^{\alpha}}{2}$, where $\frac{\lambda^{\alpha}}{2}$ is $SU(3)$ color generators.

The effective potential $\mathcal{U}(\Phi[A],\bar{\Phi}[A],T)$ is expressed in terms of the traced Polyakov loop $\Phi = (\mathrm{Tr}_c L)/N_C$ and its conjugate $\bar{\Phi} = (\mathrm{Tr}_c L^{\dagger})/N_C$. The Polyakov loop, L, is a matrix in color space

$$L(\vec{x}) = \mathcal{P}\mathrm{exp}\left[i\int_0^{\frac{1}{T}}\mathrm{d}\tau A_4(\vec{x},\tau)\right], \tag{2}$$

where $A_4 = iA_0$.

The temperature-dependent Polyakov loop effective potential, $\mathcal{U}(\Phi,\bar{\Phi},T)$, proposed in Ref. [39], takes the form

$$\begin{aligned}\frac{\mathcal{U}(\Phi,\bar{\Phi},T)}{T^4} &= -\frac{a(T)}{2}\bar{\Phi}\Phi+b(T)\ln\left[1-6\bar{\Phi}\Phi\right.\\ &\quad\left.+4(\bar{\Phi}^3+\Phi^3)-3(\bar{\Phi}\Phi)^2\right],\end{aligned} \tag{3}$$

where

$$a(T) = a_0+a_1\left(\frac{T_0}{T}\right)+a_2\left(\frac{T_0}{T}\right)^2,\quad b(T) = b_3\left(\frac{T_0}{T}\right)^3. \tag{4}$$

The parameters a_i, b_i, summarized in Table 1, are precisely fitted according to the result of lattice QCD thermodynamics in pure gauge sector.

The parameter $T_0 = 270$ MeV is the confinement–deconfinement transition temperature in the pure Yang–Mills theory at vanishing chemical potential [40]. In the presence of fermions, the quantum backreaction of the matter sector to the glue sector should be considered, which leads to a flavor and quark chemical potential dependence of the transition temperature, $T_0(N_f,\mu)$ [32–36]. By using

Table 1 Parameters in Polyakov effective potential given in Ref. [39]

a_0	a_1	a_2	b_3
3.51	−2.47	15.2	−1.75

renormalization group theory in Ref. [32], the form of $T_0(N_f,\mu)$ is proposed to be

$$T_0(N_f,\mu)=T_\tau e^{-1/(\alpha_0 b(N_f,\mu))}, \tag{5}$$

where

$$b(N_f,\mu)=\frac{11N_c-2N_f}{6\pi}-\beta\frac{16N_f}{\pi}\frac{\mu^2}{T_\tau^2}. \tag{6}$$

The running coupling $\alpha_0=0.304$ is fixed at the τ scale $T_\tau=1.770$ GeV according to the deconfinement transition temperature $T_0=270$ MeV of pure gauge field with $N_f=0$ and $\mu=0$. When fermion fields are included, T_0 is rescaled to 208 MeV for 2 flavor and 187 MeV for 2 + 1 flavor at vanishing chemical potential. The parameter β in Eq. (6) governs the curvature of $T_0(\mu)$ as a function of quark chemical potential.

With the consideration of the chemical potential dependence of Polyakov loop potential, this improved PNJL model is named the μPNJL model. We then replace the T_0 with $T_0(N_f,\mu)$ in the Polyakov loop potential given in Eq. (4). The thermodynamical potential of quark matter in the μPNJL model within the mean field approximation can be derived then as

$$\begin{aligned}\Omega=&\mathcal{U}(\bar\Phi,\Phi,T)+G(\phi_u+\phi_d)^2-2\int_\Lambda\frac{\mathrm{d}^3\boldsymbol{k}}{(2\pi)^3}3(E_u+E_d)\\&-2T\sum_{u,d}\int\frac{\mathrm{d}^3\boldsymbol{k}}{(2\pi)^3}\Big[\ln(1+3\Phi e^{-(E_i-\mu_i)/T}\\&+3\bar\Phi e^{-2(E_i-\mu_i)/T}+e^{-3(E_i-\mu_i)/T})\Big]\\&-2T\sum_{u,d}\int\frac{\mathrm{d}^3\boldsymbol{k}}{(2\pi)^3}\Big[\ln(1+3\bar\Phi e^{-(E_i+\mu_i)/T}\\&+3\Phi e^{-2(E_i+\mu_i)/T}+e^{-3(E_i+\mu_i)/T})\Big],\end{aligned} \tag{7}$$

where $E_i=\sqrt{\boldsymbol{k}^2+M_i^2}$ is energy-momentum dispersion relation of quark flavor, i, and μ_i is the corresponding quark chemical potential.

The dynamical quark masses and quark condensates are coupled with the following equations

$$M_i=m_0-2G(\phi_u+\phi_d), \tag{8}$$

$$\phi_i=-2N_c\int\frac{\mathrm{d}^3\boldsymbol{k}}{(2\pi)^3}\frac{M_i}{E_i}\big(1-n_i(k)-\bar n_i(k)\big), \tag{9}$$

where $n_i(k)$ and $\bar n_i(k)$

$$n_i(k)=\frac{\Phi e^{-(E_i-\mu_i)/T}+2\bar\Phi e^{-2(E_i-\mu_i)/T}+e^{-3(E_i-\mu_i)/T}}{1+3\Phi e^{-(E_i-\mu_i)/T}+3\bar\Phi e^{-2(E_i-\mu_i)/T}+e^{-3(E_i-\mu_i)/T}}, \tag{10}$$

$$\bar n_i(k)=\frac{\bar\Phi e^{-(E_i+\mu_i)/T}+2\Phi e^{-2(E_i+\mu_i)/T}+e^{-3(E_i+\mu_i)/T}}{1+3\bar\Phi e^{-(E_i+\mu_i)/T}+3\Phi e^{-2(E_i+\mu_i)/T}+e^{-3(E_i+\mu_i)/T}} \tag{11}$$

are modified Fermion distribution functions of quark and antiquark. The values of ϕ_u,ϕ_d,Φ, and $\bar\Phi$ can be determined by minimizing the thermodynamical potential,

$$\frac{\partial\Omega}{\partial\phi_u}=\frac{\partial\Omega}{\partial\phi_d}=\frac{\partial\Omega}{\partial\Phi}=\frac{\partial\Omega}{\partial\bar\Phi}=0. \tag{12}$$

All the thermodynamic quantities relevant to the bulk properties of quark matter can be obtained from Ω. Particularly, we note that the pressure and energy density should be zero in the vacuum. In the calculation a cutoff, Λ, is implemented in 3-momentum space for divergent integrations. $\Lambda=651$ MeV, $G=5.04\,\mathrm{GeV}^{-2}$, and $m_{u,d}=5.5$ MeV will be taken by fitting the experimental values of pion decay constant $f_\pi=92.3$ MeV and pion mass $m_\pi=139.3$ MeV [21].

3 Results and discussion

In this section, we present the properties of quark matter in the improved PNJL model with a chemical potential-dependent Polyakov effective potential which effectively reflects the backreaction of matter sector to glue sector at non zero chemical potential. In the original PNJL model, the parameter T_0, describing the confinement–deconfinement transition temperature in the pure Yang–Mills theory at vanishing chemical potential, is a constant. When the backreaction of matter sector to glue sector is included, T_0 will show a feature of chemical potential dependence, as presented in Fig. 1.

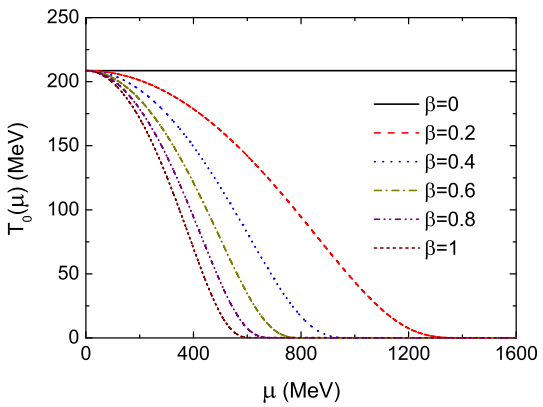

Fig. 1 (Color online) $T_0(\mu)$ as a function of μ with various β from 0 to 1. The case $\beta=0$ corresponds to the standard PNJL model

To mimic the strength of the quantum backreaction of matter sector to glue sector, different values of β are used in the calculation for a tentative study. In the case of $\beta = 0$, corresponding to the standard PNJL model, in which only the contribution from gauge field to Polyakov loop potential is considered, $T_0(\mu) = 208$ MeV is a constant, as shown with the solid line in Fig. 1. The dotted lines show the results for $\beta \neq 0$. These lines manifest that $T_0(\mu)$ is sensitive to the value of β which reflects the strength of quantum backreaction of matter sector to glue sector at finite chemical potential. This figure indicates that the deconfinement temperature decreases with the increase of β.

We plot in Fig. 2 the values of Polyakov loop Φ and $\bar{\Phi}$ as functions of baryon density for various β at $T = 20$ MeV. In the original PNJL model (the case $\beta = 0$), Φ and $\bar{\Phi}$ always take small values at low temperature. This means that quarks are confined, even in the high density region where the chiral symmetry is restored. This forms the so-called quarkyonic phase at a low T and high density region. However, with the consideration of quark quantum backreaction to glue sector at finite chemical potential, quark confinement–deconfinement phase transition can occur at low T, as shown by the dotted lines with different values of β. If we take the standard that Φ or $\bar{\Phi} = 0.5$ marks the happening of deconfinement transition, as adopted in Refs. [20, 23], we find the deconfinement transition density moves to a lower one for a larger β. However, we should note that when $\beta > 1.2$ is taken in the calculation, unphysical results will be derived with too small deconfined baryon density where the chiral symmetry is still breaking. For the relevant study, one can also refer to Refs. [35–37].

We plot the full QCD phase diagram in Fig. 3 for different values of $\beta = 0, 0.25, 0.5$, and 0.75 to show the influence of quantum backreaction of matter sector to glue sector on the QCD phase structure. In this figure, the red

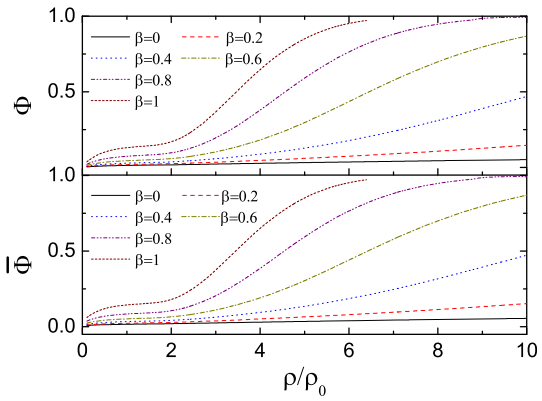

Fig. 2 (Color online) Polyakov loop Φ and $\bar{\Phi}$ as functions of baryon density, ρ_B, for different β at $T = 20$ MeV

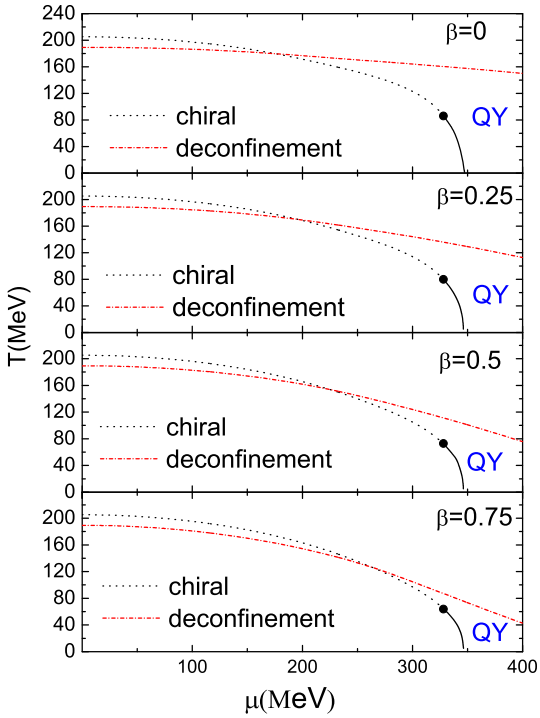

Fig. 3 (Color online) QCD phase diagram with different parameter β. "QY" in the figure means quarkyonic phase. the *red dash-dotted line* in each panel describes the confinement–deconfinement phase transition, and the *dotted and solid lines* are the chiral phase transition lines. The *dotted line* at high temperature means the chiral phase transition is a smooth crossover. The chiral phase transition at low temperature as shown with the *black solid line* is the first order. The *solid dot* is the end point of the first-order phase transition

dash-dotted line in each panel describes the confinement–deconfinement phase transition. The dotted and solid lines are the chiral phase transition lines. The dotted line at high temperature in each panel means the chiral phase transition is a smooth crossover, and the chiral phase transition at low temperature is the first order, as shown with the black solid line. The solid dot is the end point of the first-order phase transition for each β.

In the upper panel, the case of $\beta = 0$ is the phase diagram derived in the standard two-flavor PNJL model. We can see that there exist a quite large region of quarkyonic matter (marked QY in Fig. 3), which means a phase where the chiral symmetry restores, but quarks are still confined. The appearance of quarkyonic phase in fact displays the relation between chiral restoration of quark condensate and color deconfinement in the QCD phase diagram at large chemical potential.

As indicated in Fig. 3 with different values of β, we can see that strength of quantum backreaction plays an important role on the QCD phase diagram at large chemical potential. When a larger β is taken, the first-order transition line becomes shorter and correspondingly the critical end point moves toward lower temperature and larger chemical

potential. What's more, compared with the original PNJL model, the confinement–deconfinement transition can take place at lower temperature in the improved μPNJL model, which result in a great shrink of quarkyonic phase when a larger β is taken. Once again, it demonstrates that the quantum backreaction of matter sector to glue sector at finite chemical potential is significant for the QCD phase structure. The future heavy-ion-collision experiments will provide us more hints on the QCD phase structure and provide opportunities to test the quark quantum backreaction effect.

From Fig. 3, we also notice that the critical temperatures of chiral and deconfinement phase transition at $\mu = 0$ are different. The difference is about 15 MeV in the two-flavor PNJL model. For the incoincidence of the two kinds of phase transition at zero quark chemical potential, lattice QCD still cannot provide strict limit on this aspect. For example, lattice QCD simulation shows the difference of the critical point of the two phase transition is 25 MeV in Ref. [8], 18 MeV in Ref. [9]. But in Ref. [6], the lattice calculation shows that the two phase transitions happen simultaneously. More lattice QCD results about the difference of the two phase transitions are compiled in Ref. [36]. Besides, Coleman and Witten conjectured that chiral and deconfinement transition should happen coincidently. In theory, this can be realized by introducing the entanglement interaction between chiral condensate and Polyakov loop, as shown in Ref. [23]. Relevant discussions can also be found in our previous study [41]. A further study involving the coincidence problem is also in progress in an improved three-flavor PNJL quark model.

4 Summary

We have studied the properties of quark matter in the improved PNJL model with the chemical potential-dependent Polyakov loop effective potential which effectively reflects, to some degree, the quantum backreaction of matter sector to glue sector at nonzero chemical potential. Compared with the original PNJL model, a superiority of the improved μPNJL model is that it can effectively describe the confinement–deconfinement transition at low T and high density region. And the QCD phase structure will be effectively modified if the strength of the quantum backreaction of matter sector to glue sector is strong. One evident variation is that the region of the so-called quarkyonic phase will be greatly reduced in the μPNJL model. It indicates that the modification to the Polyakov loop potential with the chemical potential dependence is a significant improvement in exploring the full QCD phase diagram.

References

1. S. Gupta, X. F. Luo, B. Mohanty *et al.*, Scale for the phase diagram of quantum chromodynamics. Science **332**, 1525 (2011), doi:10.1126/science.1204621
2. P. Braun-Munzinger, J. Wambach, Phase diagram of strongly interacting matter. Rev. Mod. Phys. **81**, 1031 (2009). doi:10.1103/RevModPhys.81.1031
3. K. Fukushima, T. Hatsuda, The phase diagram of dense QCD. Rept. Prog. Phys. **74**, 014001 (2011). doi:10.1088/0034-4885/74/1/014001
4. O. Kaczmarek, F. Zantow, Static quark-antiquark interactions in zero and finite temperature QCD: I. Heavy quark free energies, running coupling, and quarkonium binding. Phys. Rev. D **71**, 114510 (2005). doi:10.1103/PhysRevD.71.114510
5. C.R. Allton, S. Ejiri, S.J. Hands et al., QCD thermal phase transition in the presence of a small chemical potential. Phys. Rev. D **66**, 074507 (2002). doi:10.1103/PhysRevD.66.074507
6. M. Cheng, N.H. Christ, S. Datta et al., Transition temperature in QCD. Phys. Rev. D **74**, 054507 (2006). doi:10.1103/PhysRevD.74.054507
7. Y. Aoki, S. Borsányi, S. Dürr et al., The QCD transition temperature: results with physical masses in the continuum limit II. J. High Energy Phys. **06**, 088 (2009). doi:10.1088/1126-6708/2009/06/088
8. Y. Aokia, Z. Fodora, S.D. Katza et al., The QCD transition temperature: Results with physical masses in the continuum limit. Phys. Lett. B **643**, 46 (2006). doi:10.1016/j.physletb.2006.10.021
9. S. Borsányi, Z. Fodor, C. Hoelbling et al., Is there still any T_c mystery in lattice QCD? Results with physical masses in the continuum limit III. J. High Energy Phys. **09**, 073 (2010). doi:10.1007/JHEP09(2010)073
10. M. D'Elia, F. Sanfilippo, Thermodynamics of two flavor QCD from imaginary chemical potentials. Phys. Rev. D **80**, 014502 (2009). doi:10.1103/PhysRevD.80.014502
11. S. Ejiri, Canonical partition function and finite density phase transition in lattice QCD. Phys. Rev. D **78**, 074507 (2008). doi:10.1103/PhysRevD.78.074507
12. M.A. Clark, A.D. Kennedy, Accelerating dynamical-fermion computations using the rational hybrid Monte Carlo algorithm with multiple pseudofermion fields. Phys. Rev. Lett. **98**, 051601 (2007). doi:10.1103/PhysRevLett.98.051601
13. I.C. Clöt, C.D. Roberts, Explanation and prediction of observables using continuum strong QCD. Prog. Part. Nucl. Phys. **77**, 1 (2014). doi:10.1016/j.ppnp.2014.02.001
14. S.S. Xu, Z.F. Cui, B. Wang et al., Chiral phase transition with a chiral chemical potential in the framework of Dyson–Schwinger equations. Phys. Rev. D **91**, 056003 (2015). doi:10.1103/PhysRevD.91.056003
15. M. Buballa, NJL-model analysis of dense quark matter. Phys. Rep. **407**, 205 (2005). doi:10.1016/j.physrep.2004.11.004
16. P.C. Chu, X. Wang, L.W. Chen et al., Quark magnetar in the three-flavor Nambu–Jona–Lasinio model with vector interactions and a magnetized gluon potential. Phys. Rev. D **91**, 023003 (2015). doi:10.1103/PhysRevD.91.023003
17. G.Q. Cao, L.Y. He, P.F. Zhuang, Collective modes and Kosterlitz–Thouless transition in a magnetic field in the planar Nambu–Jona–Lasinio model. Phys. Rev. D **90**, 056005 (2014). doi:10.1103/PhysRevD.90.056005
18. D.P. Menezes, M.B. Pinto, L.B. Castro et al., Repulsive vector interaction in three-flavor magnetized quark and stellar matter. Phys. Rev. C **89**, 055207 (2014). doi:10.1103/PhysRevC.89.055207
19. J. Xu, T. Song, C.M. Ko et al., Phys. Rev. Lett. **112**, 012301 (2014). doi:10.1103/PhysRevLett.112.012301

20. K. Fukushima, Phase diagrams in the three-flavor Nambu–Jona–Lasinio model with the Polyakov loop. Phys. Rev. D **77**, 114028 (2008). doi:10.1103/PhysRevD.77.114028
21. C. Ratti, M.A. Thaler, W. Weise, Phases of QCD: lattice thermodynamics and a field theoretical model. Phys. Rev. D **73**, 014019 (2006). doi:10.1103/PhysRevD.73.014019
22. P. Costa, M.C. Ruivo, C.A. de Sousa et al., Phase diagram and critical properties within an effective model of QCD: the Nambu–Jona–Lasinio model coupled to the Polyakov loop. Symmetry **2**, 1338 (2010). doi:10.3390/sym2031338
23. Y. Sakai, T. Sasaki, H. Kouno et al., Entanglement between deconfinement transition and chiral symmetry restoration. Phys. Rev. D **82**, 076003 (2010). doi:10.1103/PhysRevD.82.076003
24. B.-J. Schaefer, M. Wagner, J. Wambach, Thermodynamics of (2+1)-flavor QCD: confronting models with lattice studies. Phys. Rev. D **81**, 074013 (2010). doi:10.1103/PhysRevD.81.074013
25. V. Skokov, B. Friman, K. Redlich, Quark number fluctuations in the Polyakov loop-extended quark–meson model at finite baryon density. Phys. Rev. C **83**, 054904 (2011). doi:10.1103/PhysRevC.83.054904
26. S. Chatterjee, K.A. Mohan, Including the fermion vacuum fluctuations in the (2+1) flavor Polyakov quark–meson model. Phys. Rev. D **85**, 074018 (2012). doi:10.1103/PhysRevD.85.074018
27. J.F. Xu, G.X. Peng, F. Liu et al., Strange matter and strange stars in a thermodynamically self-consistent perturbation model with running coupling and running strange quark mass. Phys. Rev. D **92**, 025025 (2015). doi:10.1103/PhysRevD.92.025025
28. C.J. Xia, G.X. Peng, S.W. Chen et al., Thermodynamic consistency, quark mass scaling, and properties of strange matter. Phys. Rev. D **89**, 105027 (2014). doi:10.1103/PhysRevD.89.105027
29. G.X. Peng, A. Li, U. Lombardo, Deconfinement phase transition in hybrid neutron stars from the Brueckner theory with three-body forces and a quark model with chiral mass scaling. Phys. Rev. C **77**, 065807 (2008). doi:10.1103/PhysRevC.77.065807
30. L. McLarren, R.D. Pisarski, Phases of dense quarks at large N_c. Nucl. Phys. A **796**, 83 (2007). doi:10.1016/j.nuclphysa.2007.08.013
31. Y. Hidaka, L. McLarren, R.D. Pisarski, Baryons and the phase diagram for a large number of colors and flavors. Nucl. Phys. A **808**, 117 (2008). doi:10.1016/j.nuclphysa.2008.05.009
32. B.-J. Schaefer, J.M. Pawlowski, J. Wambach, Phase structure of the Polyakov–quark–meson model. Phys. Rev. D **76**, 074023 (2007). doi:10.1103/PhysRevD.76.074023
33. T.K. Herbst, J.M. Pawlowski, B.-J. Schaefer, The phase structure of the Polyakov–quark–meson model beyond mean field. Phys. Lett. B **696**, 58 (2011). doi:10.1016/j.physletb.2010.12.003
34. T.K. Herbst, J.M. Pawlowski, B.-J. Schaefer, Phase structure and thermodynamics of QCD. Phys. Rev. D **88**, 014007 (2013). doi:10.1103/PhysRevD.88.014007
35. H. Abuki, R. Anglani, R. Gatto et al., Chiral crossover, deconfinement, and quarkyonic matter within a Nambu–Jona–Lasinio model with the Polyakov loop. Phys. Rev. D **78**, 034034 (2008). doi:10.1103/PhysRevD.78.034034
36. X.Y. Xin, S.X. Qin, Y.X. Liu, Improvement on the Polyakov–Nambu–Jona–Lasinio model and the QCD phase transitions. Phys. Rev. D **89**, 094012 (2014). doi:10.1103/PhysRevD.89.094012
37. G.Y. Shao, Z.D. Tang, M. Di Toro et al., Phase transition of strongly interacting matter with a chemical potential dependent Polyakov loop potential. Phys. Rev. D **94**, 014008 (2016). doi:10.1103/PhysRevD.94.014008
38. V.A. Dexheimer, S. Schramm, Novel approach to modeling hybrid stars. Phys. Rev. C **81**, 045201 (2010). doi:10.1103/PhysRevC.81.045201
39. S. Rößner, C. Ratti, W. Weise, Polyakov loop, diquarks, and the two-flavor phase diagram. Phys. Rev. D **75**, 034007 (2007). doi:10.1103/PhysRevD.75.034007
40. M. Fukugita, M. Okawa, A. Ukava, Finite-size scaling study of the deconfining phase transition in pure SU(3) lattice gauge theory. Nucl. Phys. B **337**, 181 (1990). doi:10.1016/0550-3213(90)90256-D
41. G.Y. Shao, Z.D. Tang, M. Di Toro et al., Entanglement interaction and the phase diagram of strongly interacting matter. Phys. Rev. D **92**, 114027 (2015). doi:10.1103/PhysRevD.92.114027